Engineering and Technology Journal e-ISSN: 2456-3358

Volume 08 Issue 10 October -2023, Page No.- 2876-2886

DOI: 10.47191/etj/v8i10.10, I.F. – 7.136

Investigating Tensile Strength of Bamboo Petung (Dendrocalamus Asper) Treated Saltwater and Molasse Compared with Steel Rebar Reinforcement: An Experimental and Numerical Study

Bagas Subchan[1], Erno Widayanto[2], Ketut A. Wiswamitra[3]

[1,2,3] Civil Engineering Department, University of Jember, Jember, Indonesia

ABSTRACT: The use of steel leads to carbon production which can worsen global warming. An alternative material to replace steel becomes an urgent prerequisite that needs to be considered. Bamboo can be the main choice due to its characteristic biomass, environmentally friendly properties, and low cost. However, bamboo is still in deficit due to its natural properties. Therefore, its mechanical properties are demonstrated in the treatment of natural resources and biological wastes such as salt and molasses. Experimental tests and numerical simulations were performed to characterize its tensile properties. Furthermore, a nonlinear finite element analysis was built in ABAQUS and proposed with plasticity, ductile fracture, and damage modelling. The results show that simulation and experiment are in good agreement in representing bamboo and steel subjected to tensile loads. The use of bamboo as a substitute for steel can be considered an application of steel reinforcement to concrete and requires further research.

KEYWORDS: bamboo; tensile strength; steel rebar reinforcement; sustainable materials; and numerical analysis

I. INTRODUCTION

Building construction requires non-renewable industrial materials, such as steel, cement, concrete, etc., which generate large amounts of carbon dioxide that cause global warming (Escamilla *et al.*, 2018; Chen *et al.*, 2022a). Sustainable buildings can be an urgent aspect of reducing carbon emissions worldwide (Salzer *et al.*, 2016). Steel is the second largest source of CO_2 emissions after cement in Indonesia. It was found that rebar production generates 8,196 Gg Co2e (14.8%), followed by 28,710 Gg Co2e (51.9%) for cement (Agung Sugardiman *et al.*, 2018). Rebar has proven to be a non-renewable, unsustainable, and expensive material, leading to global emissions and a global resource crisis. Biomass materials, especially bamboo, can be a top choice for sustainable construction by replacing steel as reinforcement for concrete. Bamboo has fast growth properties that have been analysed to effectively sequester carbon, especially in well-managed forests (Liu and Yen, 2021). Bamboo has been shown to have a tensile strength greater than that of wood (Kelkar *et al.*, 2023) and 25% greater than that of grade 60 mild steel (Qaiser *et al.*, 2020).

Bamboo still has weaknesses when used naturally or plain: it easily absorbs liquid and deteriorates over time. Bamboo expansion causes several factors that lead to cracks and voids in concrete, thereby reducing the adhesion and tensile strength of bamboo to concrete (Chen *et al.*, 2022b). Many researchers have agreed that its performance is improved by mold resistance and increased tensile strength. One way to inhibit fungal growth is treatment with chitosan-copper complex, boron-boric acid (Wahab, Sudin and Yunus, 2010; Sun *et al.*, 2012) and Ag/TiO2/PDA (polydopamine). (Liu *et al.*, 2019). On the other hand, an improvement in tensile strength was demonstrated by using degassed epoxy resin in a vacuum furnace with a yield between 480 and 550 MPa (Dessalegn *et al.*, 2022). Muhtar et al., 2019 also found that using Sikadur and pipe clamps can prevent bamboo from absorbing water and sliding due to friction with concrete. In this study, we are trying to use salt and molasses to improve tensile strength and Mowilex (wood paint) to waterproof bamboo. It was revealed that salt-treated bamboo soaked for 3 days performed better than soaked for 7/14 days (Noverma, Elok Hapsari and Yusrianti, 2020). The authors also suggested the use of molasses as an alternative to epoxy adhesion due to its non-sustainable material and expensive properties. Molasses was used in a 2022 study by Syahfitri and colleagues as a binder for lightweight composite tiles based on sorghum bagasse as the main ingredient. Research results by Syahfitri et al., 2022 show that high molasses content increases the internal bonding/adhesion performance of composite tiles. Referring to these references, the author will combine the processing of bamboo with a combination of saltwater and molasses (in addition to binding the bamboo fibers).

In summary, this study aimed to investigate the mechanical strength properties of bamboo compared to steel rebar. It is determined whether untreated bamboo and salt/salt + molasses treated bamboo maintain its properties. The bamboo sample size is in accordance with ISO 22157. Finally, its performance is used and evaluated by numerical study using ABAQUS for validation by numerical analysis.

II. MATERIALS

2.1. Bamboo

Petung bamboo *(Dendrocalamus asper)* was used in this experiment and is found in the Jember region of East Java, Indonesia. The optimal age of bamboo can be around 3 to 4 years old (Lee *et al.*, 2022), specimens were used at the age of 3 years. Javadian et al., 2019 also revealed that high-yielding natural bamboo obtained from the species Petung/*Dendrocalamus Asper* (Java) has a tensile capacity of 268–340 MPa in walls of 6–12 mm thickness and lines tube glass from 110 to 130 mm. Meanwhile, the diameter of the bamboo sample tube is 140mm and the thickness is 10-12mm.

2.2. Steel Rebar

The deformed rebars were used for comparison with the bamboo sample. The rebars in this study were commercially supplied and obtained from Mega Baja Jember, Jember, East Java, Indonesia. The diameter of the reinforcement is 10 mm. Reinforcement specifications are based on the attached product list in Table 1.

Spesification:

SNI 2052:2017 – BJTS 280

Table 1. Specification of steel rebar based on catalogue product.

Chemical composition (%)				
C	*Si*	*Mn*	*P*	*S*
0.25%	*0.21%*	*0.65%*	*0.025%*	*0.032%*
Tensile test			***Bending test***	
Yield point	***Tensile strength***	***Elongation***	***Bend diameter***	***Bend angle***
401 MPa	*590 MPa*	*18%*	*3.5 x D*	*180º*

III. METHODS

This study was conducted methodically as follows (shown in Fig 1):

1. Preparation of Bamboo
2. Experimental Investigation
3. Numerical Investigation
4. Validation

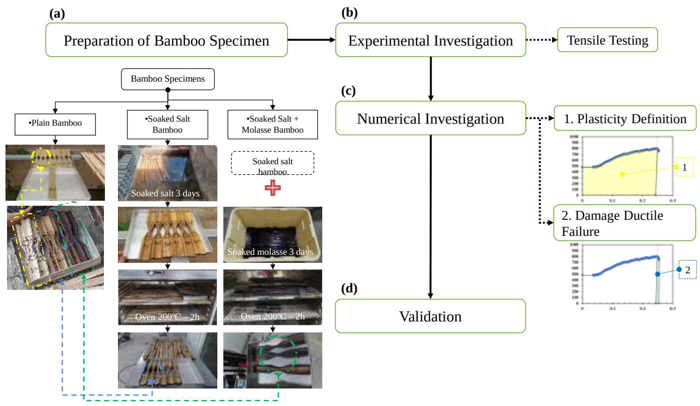

Figure 1. (a) Bamboo preparation process; (b) Experimental testing; (c) Numerical investigation; and (d) Validation.

3.1. Method of Sample Preparation

3.1.1.Bamboo

Sample preparation depends on the different bamboo treatments. Bamboo processing is divided into 3 types: natural bamboo, salt-soaked bamboo, salt-soaked bamboo and molasses-treated bamboo (Figure 1a). The design of the bamboo samples was tested using ISO 22157. Dimensions (in mm) and geometry are shown in Figure 2.

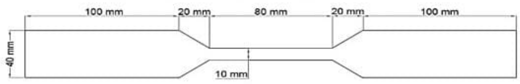

Figure 1. Bamboo specimen geometry is based on ISO 22157 standard.

3.1.2.Saltwater Treatment

Saltwater treatment of bamboo strips is done by soaking in salt solution (with a solution ratio of 0.75%) for 3 days. Salt was purchased from a local market in Jember, Indonesia. After soaking in saltwater solution, the sample was dried at 200 ºC for 2 hours. The reason for choosing this ratio is because studies reveal that bamboo has ideal performance when heated to 180°C for 1-2 hours (Bui, Grillet and Tran, 2017) and reduces performance when processed at temperatures up to 220°C (Cui *et al.*, 2023).

3.1.3.Saltwater Treatment

During the salt and molasses treatment process, the treated bamboo is further salted with the addition of molasses submerged in water and dried at 200 ºC for 2 hours. For more information, the molasses was purchased from the local market in Jember, Indonesia and pure from the Semboro sugarcane refinery.

3.1.4.Steel Rebar

Reinforcement geometry model using SNI 2052:2017 standards (shown in figure 3).

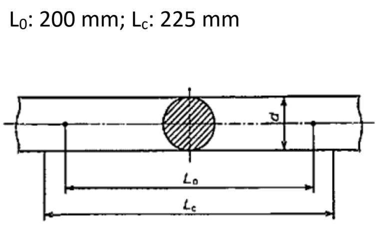

Figure 2. Geometry of specimen steel rebar based on SNI 2052:2017 standard.

3.2. Methods of Testing

In this study, the tensile strength of steel reinforcement and bamboo was determined using the universal testing machine GOTECH – GT-7001-LC50 with the parameters of speed 20-100 mm/min. The configuration of the tensile testing machine used in this study is shown in Figure 4. The bamboo and steel bars are held in the experimental machine and the load is applied continuously. From this UTM result, stress (σ), strain (ε), cross-sectional area (A) and span length (L) were calculated using the equations. (1,2 and 3)

$$\sigma = \frac{F}{A} \quad (1)$$

$$\varepsilon = \frac{\delta}{L} \quad (2)$$

$$E = \frac{\Delta\sigma}{\Delta\varepsilon} \quad (3)$$

Figure 3. Experimental Setup - Universal Testing Machine.

3.3. Finite Element Method (FEM)

Tensile tests were applied in numerical studies with boundary conditions identical to the experimental studies. The numerical investigations in this study used ABAQUS/Explicit. Figure 5 shows the shape and boundary conditions of the sample. The test specimen handles the tension on the upper surface by adjusting the lower surface in a fixed state.

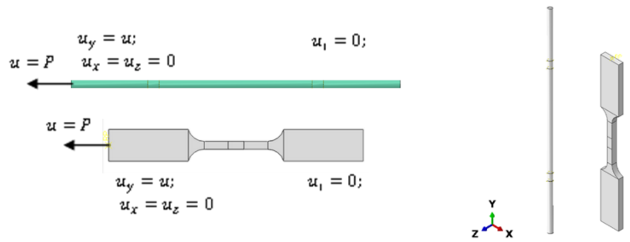

Figure 4. Boundary condition and geometry of specimen.

3.3.1. Constitutive modelling and finite element modelling

To reduce the complexity of the FEM, the tensile model is simplified to an ideal elastomer with the addition of damage failure parameters. The experimental stress-strain curve as an engineering curve cannot be applied to numerical solutions, it must be converted into a true stress-strain curve. The true stress-strain curve expressed as a power expression, an exponential expression, or a combination of both expressions can significantly influence crack simulation predictions (Standard, 2007; Zhang, Liu and Yang, 2022). The true stress-strain formula can be expressed as follows:

$$\sigma_{tru} = \sigma_{nom}(1 + \varepsilon_{nom}) \quad (4)$$

$$\varepsilon_{tru} = \ln(1 + \varepsilon_{nom}) \quad (5)$$

$$\varepsilon_{pl} = \varepsilon_{tru} - \frac{\sigma_{tru}}{E} \quad (6)$$

Where, σ_{nom} and ε_{nom} are the engineering stress strain obtained from experimental tensile test, σ_{tru} and ε_{tru} are true stress strain.

The damage failure parameters in this paper use the ductile damage criteria proposed by ABAQUS, 2006 and Li, Yuan and Liu, 2021. The plastic damage initiation criterion is a model to predict the occurrence of damage due to nucleation, growth, and coalescence of pores. in ductile metals. The model assumes that the equivalent plastic strain at the onset of failure is a triaxial function of stress and strain rate. Plastic damage can be shown in Figure 6. The equivalent plastic strain is obtained from a linear elastic fiber connected to the maximum tensile stress. This is not only the need for plastic deformation at the onset of failure but also its propagation. Some plastic destruction equations are expressed as follows:

$$\sigma = (1 - D)\bar{\sigma} \quad (7)$$

$$\bar{\varepsilon}_D^{pl}(\eta, \dot{\varepsilon}^{pl}) \quad (8)$$

where D is the overall damage variable and $\bar{\sigma}$ is the effective (or undamaged) stress tensor calculated by current gain. σ is the stress that would exist in the material if not damaged. The material loses its ability to bear force when $D = 1$. By default, an element is removed from the mesh if all part points in the integrated location have lost their carrying capacity. Meanwhile, Equation 9 determines that $\eta = -p/q$ is the triaxial stress, p is the pressure stress, q is the Mises equivalent stress, and $\dot{\varepsilon}^{pl}$ is the equivalent plastic strain rate. The criteria for determining initial damage are met when the following conditions are met:

$$\omega_D = \int \frac{d\bar{\varepsilon}^{pl}}{\bar{\varepsilon}_D^{pl}(\eta, \dot{\varepsilon}^{pl})} = 1 \quad (9)$$

where ω_D is a state variable that increases monotonically with plastic deformation. At each increment during the analysis the incremental increase in ω_D is computed as:

$$\Delta\omega_D = \frac{\Delta\bar{\varepsilon}^{pl}}{\bar{\varepsilon}_D^{pl}(\eta, \dot{\varepsilon}^{pl})} \geq 0 \quad (10)$$

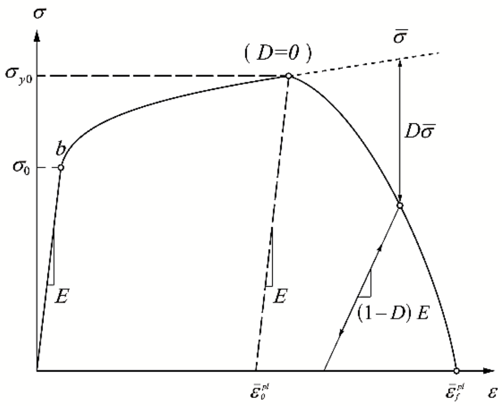

Figure 5. Ductile damage evolution.

The development of plastic damage, known as the progressive loss of material hardness leading to failure, illustrates the loss of yield strength and deterioration of elasticity. This ductility curve can be expressed in terms of fracture energy starting from the onset of failure until failure. Fracture energy can be expressed as follows:

$$G_f = \int_{\bar{\varepsilon}_D^{pl}}^{\bar{\varepsilon}_f^{pl}} L\sigma_y d\bar{\varepsilon}^{pl} = \int_0^{\bar{u}_f^{pl}} \sigma_y d\bar{u}^{pl} \quad (11)$$

This expression gives the definition of the equivalent plastic displacement, $\bar{u}^{pl}$, which is the conjugate crack work of the elastic limit after the onset of failure (work per unit surface of the crack). Before dealing damage $\bar{u}^{pl} = 0$; After starting to deal damage, $\bar{u}^{pl}$ is determined as follows:

$$\bar{u}^{pl} = L\dot{\varepsilon}^{pl} \quad (12)$$

where L is the characteristic length of the element.

The evolution of the failure variable with relative plastic displacement can be determined in tabular, linear, or exponential form. Instantaneous failure will occur if the plastic displacement at the time of failure, $\bar{u}_f^{pl}$, is determined to be 0; however, this option is not recommended and must be used with caution as it causes a sudden stress to drop at the material point and can lead to dynamic instability.

Determining the characteristic length is based on the shape of the element. In this study, the bamboo sample uses solid elements, and the steel reinforcement uses shell elements. The characteristic length can be obtained for solid elements we use the cube root of the volume of the integration point and for shell elements we use the square root of the area of the integration point. To determine the spread or evolution of damage, he divided three methods: linear, tabular, and exponential (depicted in Fig 7). This study uses the linear method to determine plastic damage, the linear equation is expressed as follows:

$$\dot{d} = \frac{L\dot{\varepsilon}^{pl}}{\bar{u}_f^{pl}} = \frac{\dot{u}^{pl}}{\bar{u}_f^{pl}} \quad (13)$$

This definition ensures that when the effective plastic displacement reaches the value $\bar{u}^{pl} = \bar{u}_f^{pl}$, the stiffness of the material will be completely reduced ($d = 1$).

$$\bar{u}_f^{pl} = \frac{2G_f}{\sigma_{y0}} \quad (14)$$

and σ_{y0} is the value of the yield stress at the time when the failure criterion is reached. Therefore, the model becomes equivalent to that shown in Figure 7(b). The model ensures that the energy dissipated during the damage evolution process is equal to only if the effective response of the material is perfectly plastic (constant yield stress) beyond the onset of damage.

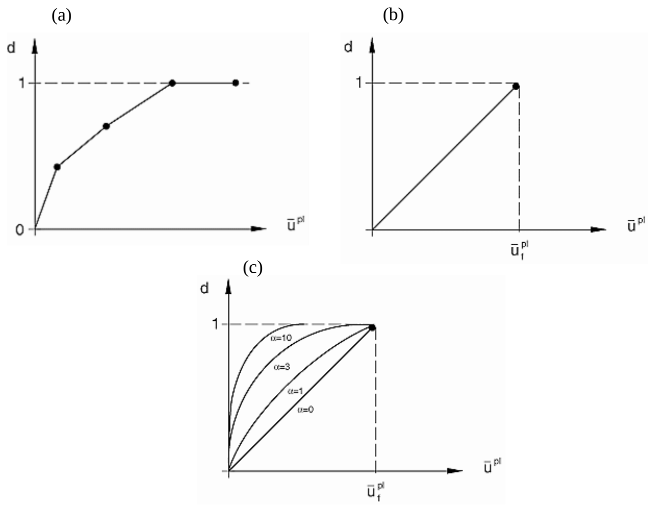

Figure 6. Definitions of damage evolution based on plastic displacement (a) tabular, (b) linear, and (c) exponential.

3.3.2. Validation of the finite element model

FEM validation uses stress and strain distributions, as well as load and strain capacities. The calculation and comparison between analytical results and experimental results use the following equation:

$$Error\ Check = \frac{\text{ABAQUS Analysis Result} - \text{Test Result}}{\text{ABAQUS Analysis Result}} * 100 \quad (14)$$

IV. RESULTS AND DISCUSSION

In this section, first, the experimental results are shown and discussed. Then, the comparison between the experimental and numerical results is presented.

4.1. Experimental results

The experimental stress-strain relationship for the bamboo samples is shown in Figure 8 (Figure 8a. plain bamboo; b.

salt-soaked bamboo; and c. salt and molasse-soaked bamboo). The tensile strength can be obtained from this curve, which means that Petung bamboo has an average tensile strength of 139.55 MPa, 133.2026 MPa and 167.8016 MPa for plain bamboo, salt-soaked bamboo, and salt and molasse-soaked bamboo, respectively. Meanwhile, the reinforcement has a stress-strain curve as shown in Figure 9, meaning the reinforcement has a tensile strength of 626.4037 MPa. All the steel and bamboo samples had yield strength and tensile strength shown in Table 2. The summary report that bamboo treated with pickling salt and molasses improved its tensile strength by about 16.84%, while salt treatment reduced it by 4.8%. The tension behaviour of bamboo showed irregularities before reaching the maximum stress. This irregular curve reflects the fact that bamboo has a different failure mechanism, namely shear behaviour leading to shear failure. However, the durability of bamboo should still be taken as evidence of its good durability. On the other hand, the tensile strength of bamboo compared to steel is still sufficient, but to apply it to concrete, the tensile area must be compared with the tensile strength to be able to take this into account.

Images of all samples after tensile testing are shown in Figure 10. The observed damage modes were approximately the same for bamboo, as they were for steel. In the case of broken bamboo, all have shear slippage cracks, this means that the bamboo has broken at the connecting fiber and is slipping due to cutting.

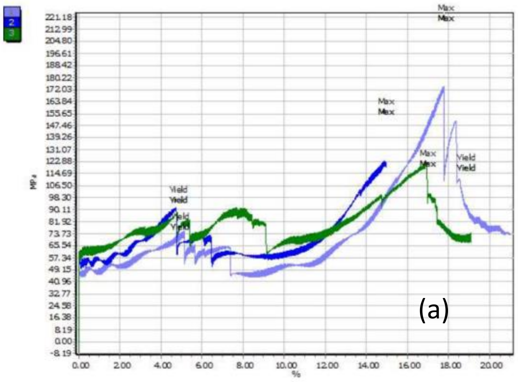

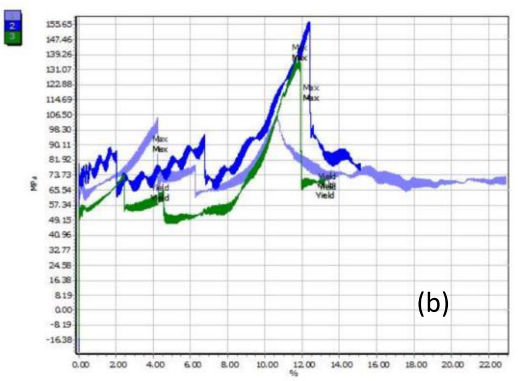

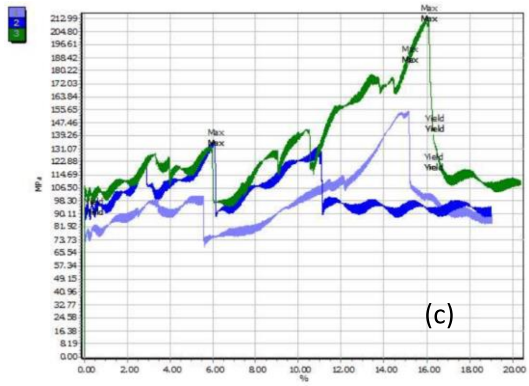

Figure 7. a. Tensile strength of plain bamboo; b.-soaked salt treatment bamboo; and c.-soaked salt and molasse treatment bamboo.

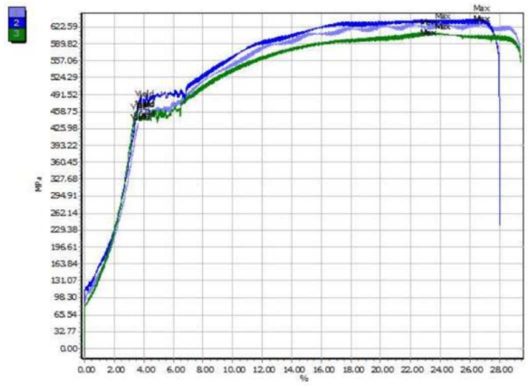

Figure 8. The tensile strength of deformed steel rebar diameter 10 mm.

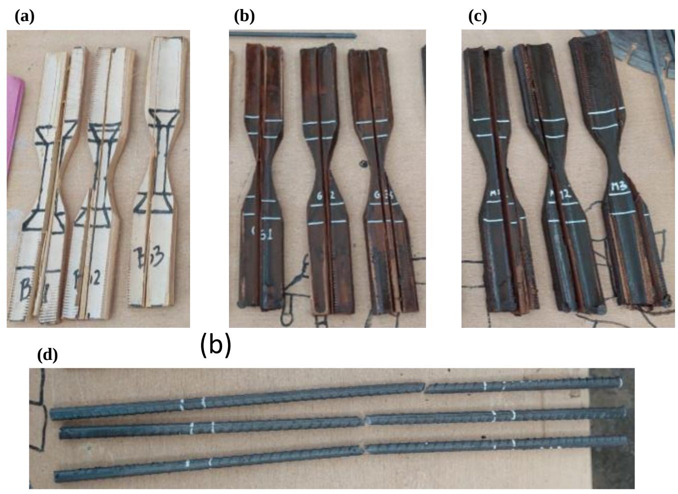

Figure 9. Failure of specimens (a) Plain bamboo; (b) salted treated bamboo; (c) salted and molasse treated bamboo; and (d) steel rebar.

Table 2. Yield strength and tensile strength of bamboo and steel rebar.

	Material		Area (mm^2)	Yield stress (MPa)	Tensile strength (MPa)	Displacement (mm)	Elongation (%)
1.	Plain bamboo (B)	B1	140.22	93.81	174.21	16.812	21.04
		B2	141.20	75.76	123.14	11.968	14.98
		B3	110.73	78.59	121.29	15.272	19.09

	Average		**130.72**	**82.72**	**139.55**	**14.68**	**18.37**
2.	Soaked salt bamboo (S)	S1	95.32	73.14568	104.8509	18.34	22.93746
		S2	83.59	85.35935	157.2172	12.076	15.12446
		S3	114.02	67.42249	137.5397	10.58	13.24211
	Average		**98.64**	**75.31**	**133.21**	**13.67**	**17.101**
3.	Soaked salt + molasse bamboo (M)	M1	105.71	98.46255	154.8116	15.212	19.0452
		M2	86.78	91.39919	135.5453	15.188	19.01053
		M3	87.41	143.3949	213.0479	16.3	20.40372
	Average		**93.30**	**111.09**	**167.80**	**15.57**	**19.486**
4.	Steel D10	D10 1	80.28	459.1918	629.9339	58.86	29.43158
		D10 2	81.47	470.5396	637.5449	56.04	28.01981
		D10 3	81.31	445.5574	611.7322	58.93	29.46254
	Average		**81.02**	**458.56**	**626.40**	**57.94**	**28.971**

4.2. Numerical investigations

This section compares the numerical simulation results with experimental results on the stress-strain and force-displacement relationships. Before entering results, ABAQUS entries containing material definitions will be presented. The data used to convert experimental results is explained in section 4.1. The experimental data is converted into a true stress-strain curve. Specifically, the bamboo tensile strength curve has irregularities, so ideally, the bamboo tensile strength curve uses the simplified bilinear stress-strain curve. Converting the actual stress-strain relationship of the sample and calculating fracture ductile is attached in Appendix 1. After calculation, we obtain synthetic data to determine elasticity and actual yield limit, actual tensile capacity, and modelled ductile fracture (see Table 3).

Table 3. Numerical simulation inputs.

	Material	**Modulus Elasticity**	**True yield strength (MPa)**	**True tensile strength (MPa)**	**Plastic strain damage initiation**	**Fracture Energy**	**Plastic strain damage failure**
		E			$\bar{\varepsilon}_D^{pl}$	Gf	$\bar{u}_f^{pl}$
1.	Plain bamboo	19,185.54	49.048	205.907	0.142	22.22569962	0.215880799
2.	Salted treatment bamboo	28,156.14	79.058	172.220	0.1045	6.742969722	0.078306421
3.	Salted+Molasse treated bamboo	21,772.03	106.106	248.052	0.1258	23.34685916	0.188241273
4.	Steel D10	200,000	478.35	798.66	0.244	10.86475698	0.027207367

4.2.1. Tensile stress and strain distribution

The σ-ε curves obtained from experiments and numerical simulations are compared to verify the contribution of the FEA modelling methods. The σ-ε curve of bamboo is shown in Fig. 10a–c, while the reinforcing bars are shown in Fig. 10d. This is clearly shown by the numerical analyses in Fig. 10a–d: the stress-strain distributions of bamboo and steel are almost the same. The numerical results of bamboo show that bamboo reaches an elastic stage until it reaches yield stress, a maximum stress near the experiment, and a ductile behaviour that shows its failure. On reinforcing bars, the maximum stress at the outlet of the specimen occurs earlier than the experimental maximum stress and ductile failure properties develop later.

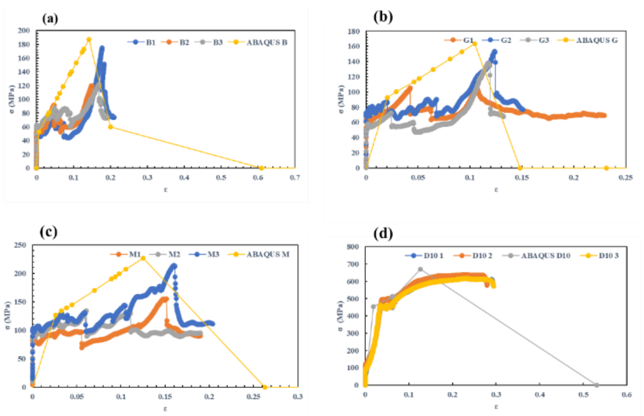

Figure 10. Stress and strain distribution (a). Plain bamboo; (b). Salted treated bamboo; (c). Salted and molasse treated bamboo; (d). Steel D10.

4.2.2. Load-carrying capacity and deformation

Figure 11a–c shows the F-Δ curve for the bamboo sample and Figure 11d for the steel reinforcement; The ultimate load F obtained by ABAQUS with the experimentally obtained average breaking load of the sample is compared in Table 4. These results confirm the accuracy and reliability of using the fracture model ABAQUS plasticity and ductility on the tensile behaviour of bamboo and steel. The results show that this method agrees well with experimental results with errors ranging from 8.13% to 26.44% for bamboo and 3.47% for steel. Based on this, the proposed FEA modelling method can generally accurately predict the structural response of bamboo and steel when subjected to tensile loading.

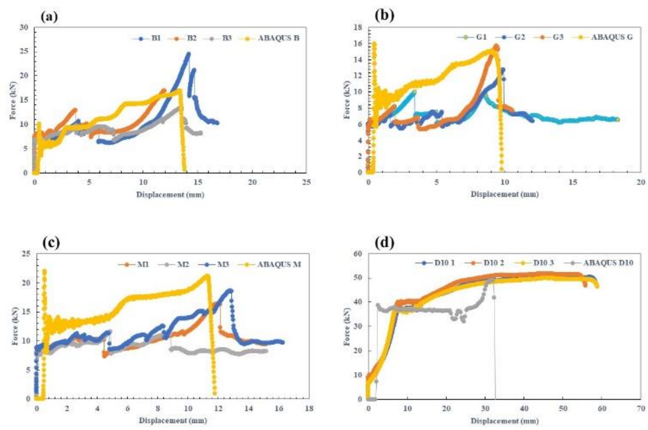

Figure 11. Comparison between experimental and numerical force-displacement curves (a). Plain bamboo; (b). Salted treated bamboo; (c). Salted and molasse treated bamboo; (d). Steel D10.

Table 4. Comparison of maximum force F for samples plain bamboo (B), salted treated bamboo (G), salted and molasse treated bamboo (M), and steel rebar (D10).

	Sample		Experiment (kN)		FEM (kN)	Error (%)
			F_{exp}	ΔF_{exp}	F_{num}	
1.	Plain bamboo	B1	24.52			
		B2	16.95	18.31	16.93	-8.13%
		B3	13.47			
2.	Salted treatment bamboo	S1	10.03			
		S2	12.81	12.86	15.12	14.95%
		S3	15.74			
3.	Salted+Molasse treated bamboo	M1	16.41			
		M2	11.64	15.58	21.18	26.44%
		M3	18.69			
4.	Steel D10	D10 1	50.75			
		D10 2	51.65	50.77	49.0717	-3.47%
		D10 3	49.92			

4.2.3. Damage propagation investigation

Figures 13 and 14 illustrate the predicted damage levels on bamboo and steel samples. The steel has similar fracture behaviour that exhibits tensile fracture starting from a sample with a weak point. Numerical studies of bamboo show intolerance behaviour under tension, while experimental testing shows slippage under shear. It can be concluded that the numerical study of bamboo requires a complete definition of the material, including the elastic modulus in terms of 3-matrix/anisotropy behaviour and shear behaviour.

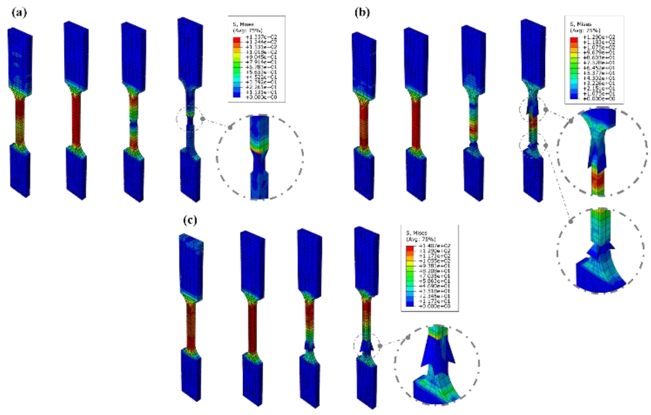

Figure 12. Failure of tensile bamboo specimen (a) Plain bamboo; (b) Salted treated bamboo; and (c) Salted and molasse treated bamboo.

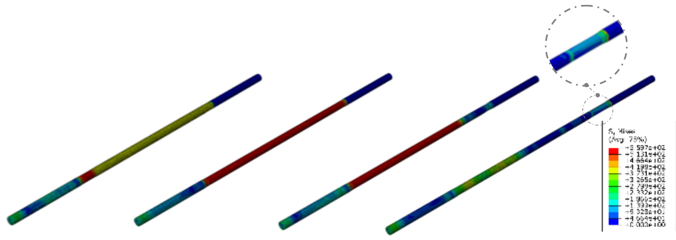

Figure 13. Failure of tensile steel rebar specimen.

CONCLUSIONS

In this paper, bamboo and steel tensile tests were investigated to evaluate the mechanical properties of treated bamboo compared to steel. Experimental tests were performed, and finite element models were performed to determine its material by numerical methods. The following conclusions were drawn from the study:

Salt/salt + molasses treatment on bamboo has little effect on tensile properties. It was found that salt and molasses soaking improved the tensile strength by about 16.84%, while salt pickling treatment reduced it by 4.8%.

Simulation results show that the stress-strain displacement from the numerical methods outputs nearly the same as the experimental method, while the steel exhibits an earlier peak stress and a later fracture behaviour.

The force displacement in the simulation can accurately predict bamboo and steel when subjected to tensile load. The results were almost identical to the experimental results, with the additional information that the steel suffered ductile failure earlier than the experimental results.

In the bamboo failure section occurred due to shear failure while numerical data showed tension, while steel failure was predicted equally well between the numerical and experimental values.

Limitation and future scope of work

In the present work, tension tests on bamboo and steel, experimental and numerical evaluation were derived. Numerical investigations using plasticity and ductile fracture modelling, show its accurate and reasonable use. Furthermore, it requires further developments, such as comparing the ductile fracture and damage model with Hashin damage, which identifies the material as anisotropic layered material. The application of bamboo to concrete such as beams also needs to be researched further to know the difference in performance compared to steel and whether it gives good results or not.

Disclosure statement

No potential conflict of interest was reported by the author(s).

ORCID

Bagas Subchan (0000-0003-3349-6105) (orcid.org)

Appendix 1

In this section, calculation of converting engineered stress-strain curve into true stress-strain curve is presented. True stress-strain curve obtained with initiation on yield tensile strength. This calculation is depending on equation 4-6.

Steel:

In instances, where:

$\varepsilon_{nom} = 0.03815$, $\sigma_{nom} = 462.3425$, and $E = 200{,}000$

$\varepsilon_{tru} = \ln(1+\varepsilon_{nom}) = \ln(1+0.03815) = 0.03744$

$\sigma_{tru} = \sigma_{nom}(1+\varepsilon_{nom}) = 462.3425(1+0.03815) = 479.9808$

$\varepsilon_{pl} = \varepsilon_{tru} - \frac{\sigma_{tru}}{E} = 0.03744 - \frac{479.9808}{200{,}000} = 0.035040379$

$\varepsilon_{nom} = 0.1295$, $\sigma_{nom} = 587.3132$, and $E = 200{,}000$

$\varepsilon_{tru} = \ln(1+\varepsilon_{nom}) = \ln(1+0.1295) = 0.12178$

$\sigma_{tru} = \sigma_{nom}(1+\varepsilon_{nom}) = 587.3132(1+0.1295) = 663.3703$

$\varepsilon_{pl} = \varepsilon_{tru} - \frac{\sigma_{tru}}{E} = 0.12178 - \frac{663.3703}{200{,}000} = 0.1184$ etc.,

To define ductile failure material, it needs $\bar{\varepsilon}_D^{pl}$, G_f, and $\bar{u}_f^{pl}$: $\bar{\varepsilon}_D^{pl}$ has defined by linear of modulus elasticity, so it obtained 0.244;

$$G_f = \int_{\bar{\varepsilon}_D^{pl}}^{\bar{\varepsilon}_f^{pl}} L\sigma_y d\bar{\varepsilon}^{pl} = 1.4 * 7.7605 = 10.8648$$

$$\bar{u}_f^{pl} = \frac{2G_f}{\sigma_{y0}} = \frac{2 * 10.8648}{798.6629} = 0.02721$$

So, the curves of true stress-strain steel D10 were:

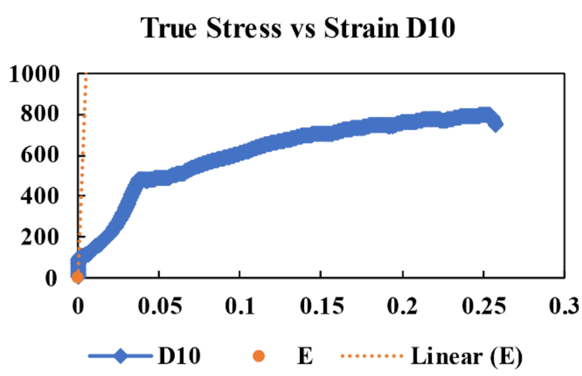

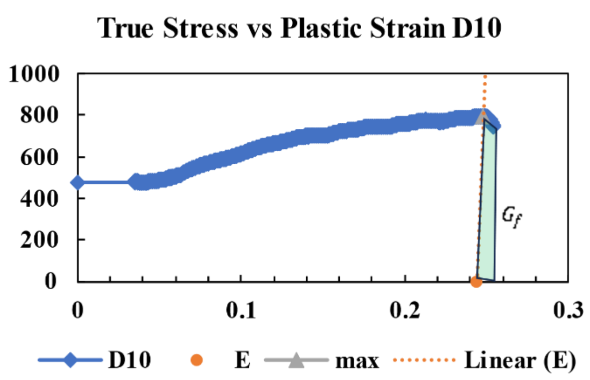

Plain bamboo:

In instances, where:

$\varepsilon_{nom} = 0.00255$, $\sigma_{nom} = 48.9231$, and $E = 48.9231/0.00255 = 19{,}185.5376$

$\varepsilon_{tru} = \ln(1+\varepsilon_{nom}) = \ln(1+0.00255) = 0.002547$

$\sigma_{tru} = \sigma_{nom}(1+\varepsilon_{nom}) = 48.9231(1+0.00255) = 49.04787$

$\varepsilon_{pl} = \varepsilon_{tru} - \frac{\sigma_{tru}}{E} = 0.002547 - \frac{49.04787}{19{,}185.5376} = -9.74823E-06 \approx 0$

$\varepsilon_{nom} = 0.1775$, $\sigma_{nom} = 174.868$, and $E = 19{,}185.5376$

$\varepsilon_{tru} = \ln(1+\varepsilon_{nom}) = \ln(1+0.1775) = 0.1634$

$\sigma_{tru} = \sigma_{nom}(1+\varepsilon_{nom}) = 174.868(1+0.1775) = 205.9071$

$\varepsilon_{pl} = \varepsilon_{tru} - \frac{\sigma_{tru}}{E} = 0.1634 - \frac{205.9071}{19{,}185.5376} = 0.152661132$

$\varepsilon_{nom} = 0.19295$, $\sigma_{nom} = 80.8729$, and $E = 19{,}185.5376$

$\varepsilon_{tru} = \ln(1+\varepsilon_{nom}) = \ln(1+0.19295) = 0.1764$

$\sigma_{tru} = \sigma_{nom}(1+\varepsilon_{nom}) = 80.8729(1+0.19295) = 96.4773$

$\varepsilon_{pl} = \varepsilon_{tru} - \frac{\sigma_{tru}}{E} = 0.1764 - \frac{96.4773}{19{,}185.5376} = 0.1714$

To define ductile failure material, it needs $\bar{\varepsilon}_D^{pl}$, G_f, and $\bar{u}_f^{pl}$:

$\bar{\varepsilon}_D^{pl}$ has defined by linear of modulus elasticity, so it obtained 0.142;

$$G_f = \int_{\bar{\varepsilon}_D^{pl}}^{\bar{\varepsilon}_f^{pl}} L\sigma_y d\bar{\varepsilon}^{pl} = 5 * 4.445139924 = 22.2257$$

$$\bar{u}_f^{pl} = \frac{2G_f}{\sigma_{y0}} = \frac{2*22.23}{205.9071} = 0.2159$$

So, the curves of true stress-strain plain bamboo were:

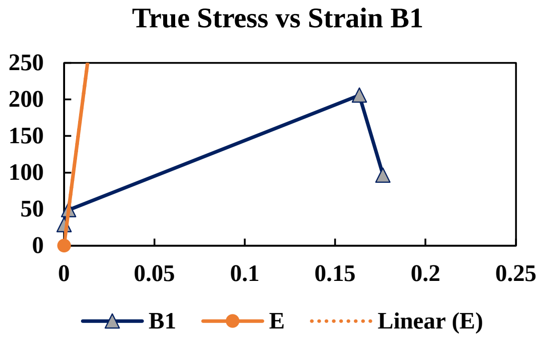

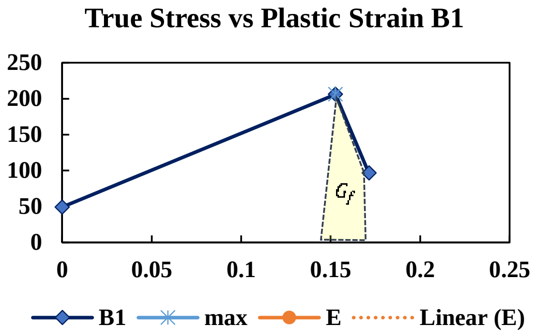

Salted treated bamboo:

In instances, where:

$\varepsilon_{nom} = 0.0028$, $\sigma_{nom} = 78.8372$, and $E = 78.8372/0.0028 = 28{,}156.13624$

$\varepsilon_{tru} = \ln(1 + \varepsilon_{nom}) = \ln(1 + 0.0028) = 0.002796$

$\sigma_{tru} = \sigma_{nom}(1 + \varepsilon_{nom}) = 78.8372(1 + 0.0028) = 79.05793$

$\varepsilon_{pl} = \varepsilon_{tru} - \frac{\sigma_{tru}}{E} = 0.002796 - \frac{79.05793}{28{,}156.13624} = -1.17527E - 05 \approx 0$

$\varepsilon_{nom} = 0.1238$, $\sigma_{nom} = 153.248$, and $E = 28{,}156.13624$

$\varepsilon_{tru} = \ln(1 + \varepsilon_{nom}) = \ln(1 + 0.1238) = 0.11672$

$\sigma_{tru} = \sigma_{nom}(1 + \varepsilon_{nom}) = 153.248(1 + 0.1238) = 172.22$

$\varepsilon_{pl} = \varepsilon_{tru} - \frac{\sigma_{tru}}{E} = 0.11672 - \frac{172.22}{28{,}156.13624} = 0.11059919$

$\varepsilon_{nom} = 0.1252$, $\sigma_{nom} = 95.8249$, and $E = 28{,}156.13624$

$\varepsilon_{tru} = \ln(1 + \varepsilon_{nom}) = \ln(1 + 0.1252) = 0.11796$

$\sigma_{tru} = \sigma_{nom}(1 + \varepsilon_{nom}) = 95.8249(1 + 0.1252) = 107.8221$

$\varepsilon_{pl} = \varepsilon_{tru} - \frac{\sigma_{tru}}{E} = 0.11796 - \frac{107.8221}{28{,}156.13624} = 0.11413$

To define ductile failure material, it needs $\bar{\varepsilon}_D^{pl}$, G_f, and $\bar{u}_f^{pl}$:

$\bar{\varepsilon}_D^{pl}$ has defined by linear of modulus elasticity, so it obtained 0.1045;

$$G_f = \int_{\bar{\varepsilon}_D^{pl}}^{\bar{\varepsilon}_f^{pl}} L\sigma_y d\bar{\varepsilon}^{pl} = 5 * 1.348593944 = 6.74297$$

$$\bar{u}_f^{pl} = \frac{2G_f}{\sigma_{y0}} = \frac{2*6.74297}{172.22} = 0.0783$$

So, the curves of true stress-strain plain bamboo were:

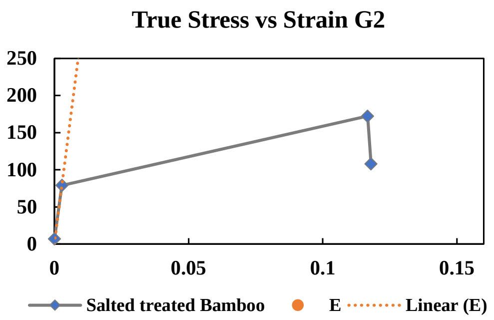

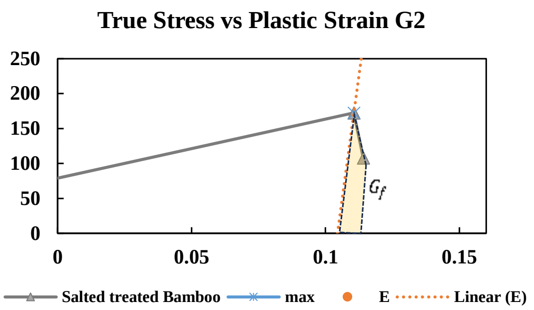

Salted and molasse treated bamboo:

In instances, where:

$\varepsilon_{nom} = 0.00485$, $\sigma_{nom} = 105.5943$, and $E = 105.5943/0.00485 = 21{,}772.0259$

$\varepsilon_{tru} = \ln(1 + \varepsilon_{nom}) = \ln(1 + 0.00485) = 0.004838$

$\sigma_{tru} = \sigma_{nom}(1 + \varepsilon_{nom}) = 105.5943(1 + 0.00485) = 106.1065$

$\varepsilon_{pl} = \varepsilon_{tru} - \frac{\sigma_{tru}}{E} = 0.004838 - \frac{106.1065}{28{,}156.13624} = -3.52459E - 05 \approx 0$

$\varepsilon_{nom} = 0.1601$, $\sigma_{nom} = 213.8199$, and $E = 21{,}772.0259$

$\varepsilon_{tru} = \ln(1+\varepsilon_{nom}) = \ln(1+0.1601) = 0.11672$

$\sigma_{tru} = \sigma_{nom}(1+\varepsilon_{nom}) = 213.8199(1+0.1601) = 248.0525$

$\varepsilon_{pl} = \varepsilon_{tru} - \frac{\sigma_{tru}}{E} = 0.11672 - \frac{248.0525}{28,156.13624} = 0.13711$

$\varepsilon_{nom} = 0.1694$, $\sigma_{nom} = 110.3993$, and $E = 21,772.0259$

$\varepsilon_{tru} = \ln(1+\varepsilon_{nom}) = \ln(1+0.1694) = 0.15649$

$\sigma_{tru} = \sigma_{nom}(1+\varepsilon_{nom}) = 110.3993(1+0.1694) = 129.1009$

$\varepsilon_{pl} = \varepsilon_{tru} - \frac{\sigma_{tru}}{E} = 0.15649 - \frac{129.1009}{28,156.13624} = 0.15056$

To define ductile failure material, it needs $\bar{\varepsilon}_D^{pl}$, G_f, and $\bar{u}_f^{pl}$:

$\bar{\varepsilon}_D^{pl}$ has defined by linear of modulus elasticity, so it obtained 0.1258;

$G_f = \int_{\bar{\varepsilon}_D^{pl}}^{\bar{\varepsilon}_f^{pl}} L\sigma_y d\bar{\varepsilon}^{pl} = 5 * 4.6694 = 23.3469$

$\bar{u}_f^{pl} = \frac{2G_f}{\sigma_{y0}} = \frac{2*23.3469}{248.0525} = 0.1882$

So, the curves of true stress-strain plain bamboo were:

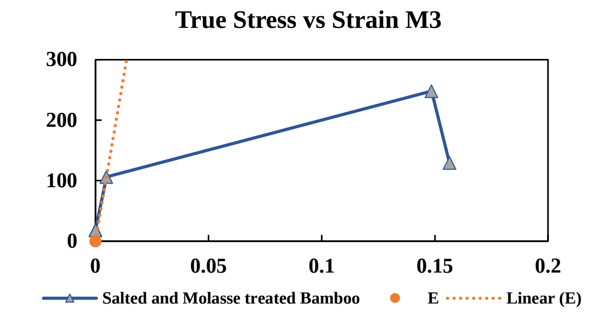

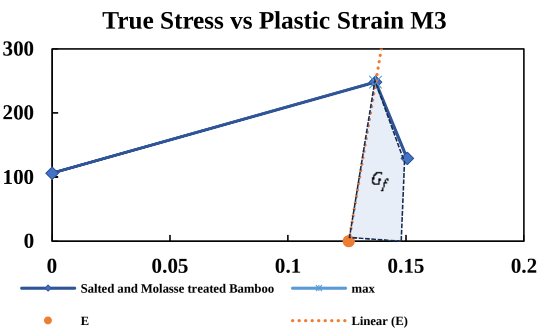

REFERENCES

1. ABAQUS (2006) *ABAQUS/CAE User's Manual 6.5 Online Documentation*. Available at: https://classes.engineering.wustl.edu/2009/spring/mase5513/abaqus/docs/v6.6/books/usi/default.htm?startat=pt03ch12s08s03.html (Accessed: 8 September 2023).
2. Agung Sugardiman, R. *et al.* (2018) *Indonesia Second Biennial Update Report - Under the United Nations Framework Convention on Climate Change*. Jakarta, Indonesia. Available at: http://www.ditjenppi.menlhk.go.id.
3. Bui, Q.B., Grillet, A.C. and Tran, H.D. (2017) 'A bamboo treatment procedure: Effects on the durability and mechanical performance', *Sustainability (Switzerland)*, 9(9). Available at: https://doi.org/10.3390/su9091444.
4. Chen, Z. *et al.* (2022a) 'State-of-the-art review on research and application of original bamboo-based composite components in structural engineering', *Structures*. Elsevier Ltd, pp. 1010–1029. Available at: https://doi.org/10.1016/j.istruc.2021.11.059.
5. Chen, Z. *et al.* (2022b) 'State-of-the-art review on research and application of original bamboo-based composite components in structural engineering', *Structures*. Elsevier Ltd, pp. 1010–1029. Available at: https://doi.org/10.1016/j.istruc.2021.11.059.
6. Cui, J. *et al.* (2023) 'Stepwise failure behavior of thermal-treated bamboo under uniaxial tensile load', *Industrial Crops and Products*, 204, p. 117313. Available at: https://doi.org/https://doi.org/10.1016/j.indcrop.2023.117313.
7. Dessalegn, Y. *et al.* (2022) 'Influence of Age and Harvesting Season on The Tensile Strength of Bamboo-Fibre-Reinforced Epoxy Composites', *Materials*, 15(12). Available at: https://doi.org/10.3390/ma15124144.
8. Escamilla, E.Z. *et al.* (2018) 'Industrial or traditional bamboo construction? Comparative life cycle assessment (LCA) of bamboo-based buildings', *Sustainability (Switzerland)*, 10(9). Available at: https://doi.org/10.3390/su10093096.
9. Javadian, A. *et al.* (2019) 'Mechanical properties of bamboo through measurement of culm physical properties for composite fabrication of structural concrete reinforcement', *Frontiers in Materials*, 6. Available at: https://doi.org/10.3389/fmats.2019.00015.
10. Kelkar, B.U. *et al.* (2023) 'Structural bamboo composites: A review of processing, factors affecting properties and recent advances', *Advances in Bamboo Science*, 3, p. 100026. Available at: https://doi.org/https://doi.org/10.1016/j.bamboo.2023.100026.
11. Lee, G.Z.X. *et al.* (2022) 'A reconnaissance study on tensile strength of bamboo based on global database', *Materials Today: Proceedings*, 64, pp. 1109–1115. Available at: https://doi.org/10.1016/j.matpr.2022.06.047.
12. Li, F., Yuan, H. and Liu, H. (2021) 'Implementation of

metal ductile damage criteria in Abaqus FEA', in *Journal of Physics: Conference Series*. IOP Publishing Ltd. Available at: https://doi.org/10.1088/1742-6596/1906/1/012058.

13. Liu, G. *et al.* (2019) 'Facile in-situ growth of Ag/TiO2 nanoparticles on polydopamine modified bamboo with excellent mildew-proofing', *Scientific Reports*, 9(1). Available at: https://doi.org/10.1038/s41598-019-53001-y.
14. Liu, Y.H. and Yen, T.M. (2021) 'Assessing aboveground carbon storage capacity in bamboo plantations with various species related to its affecting factors across Taiwan', *Forest Ecology and Management*, 481. Available at: https://doi.org/10.1016/j.foreco.2020.118745.
15. Muhtar *et al.* (2019) 'Enhancing bamboo reinforcement using a hose-clamp to increase bond-stress and slip resistance', *Journal of Building Engineering*, 26. Available at: https://doi.org/10.1016/j.jobe.2019.100896.
16. Noverma, Elok Hapsari, O. and Yusrianti (2020) *TENSILE STRENGTH OF BAMBOO AFTER PRESERVATION*.
17. Qaiser, S. *et al.* (2020) 'Flexural strength improvement in bamboo reinforced concrete beams subjected to pure bending', *Journal of Building Engineering*, 31. Available at: https://doi.org/10.1016/j.jobe.2020.101289.
18. Salzer, C. *et al.* (2016) 'Sustainability of social housing in Asia: A holistic multi-perspective development process for bamboo-based construction in the Philippines', *Sustainability (Switzerland)*, 8(2). Available at: https://doi.org/10.3390/su8020151.
19. Standard, A. (2007) 'Metallic materials—Tensile testing at ambient temperature', *AS 1391-2007, Australia* [Preprint].
20. Sun, F. *et al.* (2012) 'Mould-resistance of bamboo treated with the compound of chitosan-copper complex and organic fungicides', *Journal of Wood Science*, 58(1), pp. 51–56. Available at: https://doi.org/10.1007/s10086-011-1223-9.
21. Syahfitri, A. *et al.* (2022) 'Conversion of agro-industrial wastes of sorghum bagasse and molasses into lightweight roof tile composite', *Biomass Conversion and Biorefinery* [Preprint]. Available at: https://doi.org/10.1007/s13399-022-02435-y.
22. Wahab, R., Sudin, M. and Yunus, A.A. (2010) *Durability Performance of Gigantochloa scortechinii Through Laboratory Fungal Decay Tests**. Available at: https://www.researchgate.net/publication/292804937.
23. Zhang, Y., Liu, Y. and Yang, F. (2022) 'Ductile fracture modelling of steel plates under tensile and shear dominated states', *Journal of Constructional Steel Research*, 197. Available at: https://doi.org/10.1016/j.jcsr.2022.107469.